The AAPS Journal (2019) 21: 83
DOI: 10.1208/s12248-019-0355-5

Research Article

Theme: Natural Products Drug Discovery in Cancer Prevention
Guest Editors: Ah-Ng Tony Kong and Chi Chen

Anthocyanin Delphinidin Prevents Neoplastic Transformation of Mouse Skin JB6 P+ Cells: Epigenetic Re-activation of Nrf2-ARE Pathway

Hsiao-Chen Dina Kuo,[1,2] Renyi Wu,[1,2] Shanyi Li,[1,2] Anne Yuqing Yang,[1,2] and Ah-Ng Kong[1,2,3]

Received 22 May 2019; accepted 17 June 2019; published online 28 June 2019

Abstract. Redox imbalance is a major contributor to the pathogenesis of melanoma and nonmelanoma skin cancer. Activation of the nuclear factor E2–related factor 2 (Nrf2) antioxidant responsive element (ARE) pathway is an intrinsic defense mechanism against oxidative stress. Flavonoids such as anthocyanidins, which are found abundantly in fruits and vegetables, have been shown to activate Nrf2. However, the epigenetic and genetic mechanisms by which anthocyanidins modulate the Nrf2-ARE pathway remain poorly understood in the context of skin cancer. In this study, delphinidin, one of the most potent and abundant anthocyanidins in berries, significantly inhibited 12-O-tetradecanoylphorbol-13-acetate (TPA)–induced neoplastic cell transformation in mouse epidermal JB6 P+ cells by 69.4 to 99.4%. The mechanism was elucidated based on observations of increased ARE-driven luciferase activity and elevated mRNA and protein expression of Nrf2 downstream genes, such as heme oxygenase-1 (*Ho-1*), in JB6 P+ cells. Activation of the Nrf2-ARE pathway was correlated with demethylation of 15 CpG sites in the mouse Nrf2 promoter region between nt −1226 and −863 from the transcription start site. The reduced CpG methylation ratio in the Nrf2 promoter region was consistent with observed decreases in the protein expression of DNA methyltransferases 1 (DNMT1), DNMT3a, and class I/II histone deacetylases (HDACs). Overall, our results suggest that delphinidin, an epigenetic demethylating agent of the Nrf2 promoter, can activate the Nrf2-ARE pathway, which can be applied as a potential skin cancer chemopreventive agent.

KEY WORDS: delphinidin; DNA methylation; epigenetics; Nrf2; skin cancer.

INTRODUCTION

Skin cancer is the most common type of cancer in the USA, with 5.4 million new cases of basal and squamous cell skin cancers diagnosed in the USA in 2012 (1). Excluding basal and squamous cancers, it is estimated that there will be approximately 0.1 million new cases of skin cancer in 2019 (2). The incidence of skin cancer is rising steadily worldwide because humans are being exposed to increasing amounts of UV radiation and chemical carcinogens that initiate and promote skin neoplastic processes (1,3,4).

Many antioxidative dietary supplements, such as butylated hydroxytoluene, curcumin, silibinin, ursolic acid (5–8), and anthocyanins/anthocyanidins (9–15), have been shown to exhibit antioxidative, antiinflammatory, and antimutagenic potency against skin carcinogenesis. Anthocyanins are water-soluble flavonoids, which are the secondary metabolites

Guest Editors: Ah-Ng Tony Kong and Chi Chen

[1] Department of Pharmaceutics, Ernest Mario School of Pharmacy, Rutgers, The State University of New Jersey, 160 Frelinghuysen Road, Piscataway, New Jersey 08854, USA.
[2] Center for Phytochemical Epigenome Studies, Ernest Mario School of Pharmacy, Rutgers, The State University of New Jersey, Piscataway, New Jersey 08854, USA.
[3] To whom correspondence should be addressed. (e–mail: KongT@pharmacy.rutgers.edu)

Abbreviations: *TPA*, 12-O-tetradecanoylphorbol-13-acetate; *DMBA*, 7,12-Dimethylbenz[a]anthracene; *ARE*, Antioxidant response element; *Nrf2*, Nuclear factor E2–related factor 2; *GST*, Glutathione S-transferase; *DNMTs*, DNA methyltransferases; *HDACs*, Histone deacetylases; *HO-1*, Heme oxygenase-1; *NQO1*, NAD(P)H/quinone oxidoreductase 1; *KEAP1*, Kelch-like ECH–associated protein 1; *GCLM*, Glutamate-cysteine ligase; *MRP1*, Multidrug resistance protein 1; *SOD*, Superoxide dismutase; *ROS*, Reactive oxygen species.

derived from phenylalanine through the phenylpropanoid, flavonoid, and anthocyanin pathways (16). Different types of anthocyanin compounds are biosynthesized from dihydroflavonols through catalysis by dihydrokaempferol 4-reductase (DFR) and anthocyanidin synthase (ANS) and are modified by glycosylation and acylation (16).

While all types of anthocyanidins (aglycons of anthocyanin) demonstrate antioxidative, antiinflammatory, and apoptosis-inducing activity, delphinidin is one of the most potent compounds due to its rich abundance of hydroxyl groups on the B and C rings (Fig. 1a) (11,17). Delphinidin contributes to the intense blue colors of fruits; it is prevalent in berries and black currants (18) and can also be found in grapes, purple basil, perilla, plums, purple sage, black sorghum, corn husk, *Canna indica* flowers, purple black rice, black bean coats, and banana bracts (19–25). Delphinidin inhibits AP-1 transactivation and 12-O-tetradecanoylphorbol-13-acetate (TPA)–induced cell transformation by blocking the ERK/JNK pathway in mouse skin JB6 P+ cells (26). In the two-stage 7,12-dimethylbenz[a]anthracene (DMBA)/TPA skin carcinogenesis mouse model, delphinidin and SOD have been shown to exert a synergistic effect to prevent skin tumor progression (26,27). In addition, delphinidin shows photochemoprevention activity in human HaCaT keratinocytes and SKH-1 mice by reducing UVB-mediated oxidative stress, DNA damage, and apoptosis (28).

Nrf2 is a leucine zipper (bZIP) transcription factor that regulates the expression of antioxidant response element (ARE)–dependent genes to modulate the physiological response to the imbalance between free radicals and antioxidants (29). During responses to oxidative and electrophilic stress, Nrf2 is released from the repressor protein Keap1 and thus escapes ubiquitin–proteasome degradation (30–33). Subsequently, Nrf2 translocates from the cytoplasm to the nucleus, dimerizing with Maf family proteins to activate the ARE pathway, which upregulates the transcription of a variety of cytoprotective genes, including *Ho-1*, *Nqo1*, *Sod*, *Gclm*, and *Mrp1* (31,32,34). The antioxidative stress defense mechanism of the Nrf2-ARE pathway is a potential target for cancer prevention and therapy (32,35–37). It has been demonstrated that anthocyanins upregulate Nrf2 target antioxidative proteins and carcinogen-detoxifying enzymes to exert chemopreventive effects both *in vitro* (in rat liver clone 9 cells) (10) and *in vivo* (in a hepatocellular carcinoma rat model) (38), implying that delphinidin may be able to activate the Nrf2-ARE pathway. CpG demethylation within the Nrf2 gene promoter region associated with the induction of the Nrf2-ARE pathway has been shown to be an inhibitory mechanism of fucoxanthin against JB6 P+ skin cell transformation (39). The underlying mechanism by which antioxidants modulate the methylation patterns and the transcription of Nrf2 target genes in skin cells remains poorly understood. In this study, we investigated how delphinidin exerts antioxidative activity against skin cell neoplastic transformation by reducing CpG methylation in the Nrf2 promoter region as a candidate agent for chemoprevention.

MATERIAL AND METHODS

Chemicals, Reagents, and Antibodies

Delphinidin chloride with a purity of ≥ 97% as determined by HPLC analysis was purchased from Alkemist Labs (Costa Mesa, CA, USA). 5-Aza-deoxycytidine (5-aza), trichostatin A (TSA), Eagle's basal medium (BME), and TPA were supplied by Sigma-Aldrich (St. Louis, MO, USA). A CellTiter 96 AQueous One Solution Cell Proliferation Assay System and a luciferase assay system were provided by Promega (Madison, WI, USA). A TOPO TA Cloning Kit and One Shot™ TOP10 Chemically Competent *Escherichia coli* were purchased from Invitrogen (Waltham, MA, USA).

Cell Culture and Treatment

The mouse epidermal JB6 P+ cell line was purchased from the American Type Culture Collection (ATCC, Manassas, VA, USA). The human hepatocellular HepG2-C8 cell line was established from HepG2 cells stably transfected with the pARE-TI-luciferase construct using the FuGENE 6 method (a gift from Dr. William Fahl, University of Wisconsin) (40). The HepG2-C8 cells were grown and maintained in DMEM supplemented with 10% FBS, and the JB6 P+ cells were maintained in MEM with 5% FBS as instructed by the ATCC. The cells were first seeded and grown in plates for 24 h. Then, the cells were treated with various concentrations of delphinidin, with 0.1% DMSO as a vehicle control, or cotreated with 5-aza and TSA as a positive control in medium with 1% FBS. The treatment medium was renewed every other day. For 5-aza and TSA cotreatment, TSA (50 nM) was only added to the medium 20 h prior to harvesting the cells.

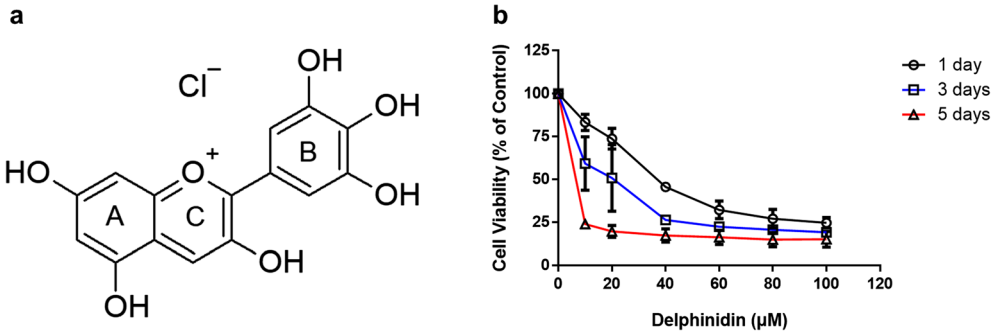

Fig. 1. **a** Chemical structure of delphinidin chloride. **b** Effect of delphinidin on the viability of JB6 P+ cells. JB6 P+ cells were treated with various concentrations of delphinidin for 1, 3, or 5 days as described in the "Material and Methods" section. Cell viability was determined with an MTS cell proliferation assay and is presented as the mean ± SEM

Cell Proliferation Assay

JB6 P+ cells were placed into a 96-well plate at a density of 3×10^3 cells per well and grown for 24 h. Then, the cells were incubated with different concentrations of delphinidin (10, 20, 40, 60, 80, or 100 μM) and with 0.1% DMSO as a vehicle control for 1, 3, or 5 days. Similarly, 5×10^3 cells/well of HepG2-C8 cells were seeded in a 96-well plate and treated with various concentrations of delphinidin (20, 40, 80, or 160 μM) or with 0.1% DMSO for 1 day. The cell culture media were renewed every other day. Cell viability was measured with the CellTiter 96® AQueous One Solution Cell Proliferation Assay System (Promega) at 490-nm absorbance as instructed by the manufacturer.

Anchorage-Independent Cell Transformation Assay

TPA-induced JB6 cell neoplastic transformation was established as indicated in previous publications (41,42). The JB6 P+ cells were seeded in 6-well plates for 24 h and then treated with different concentrations of delphinidin (5, 10, or 20 μM) or 0.1% DMSO for 3 days. Then 8×10^3 pretreated cells were subjected to an anchorage-independent cell transformation assay in 6-well plates with 0.3% BME agar (bacteriological agar, Sigma-Aldrich) as the upper agar and 0.5% BME agar as the bottom agar. The 0.3% and 0.5% BME agar were made by mixing BME supplemented with 10% FBS with 0.6% and 1% agar, respectively, in a 1:1 proportion. Cells pretreated with delphinidin were maintained in the upper agar with 10 ng/mL TPA. Cells not pretreated with delphinidin were also seeded in upper agar with and without 10 ng/mL TPA as positive and vehicle controls. After 14 days of incubation, images of the cell colonies in the soft agar were captured by a microscope camera using Nikon ACT-1 software (Version 2.20, LEAD Technologies, Charlotte, NC, USA). The colonies were quantified with the ImageJ program (Version 1.51d, NIH, Bethesda, MD, USA).

Luciferase Reporter Activity Assay

HepG2-C8 cells stably transfected with a pARE-TI-luciferase plasmid construct were used to examine ARE-driven luciferase activity, as established in our previous study (40). HepG2-C8 cells were seeded in 12-well plates at a density of 1×10^5 cells/well and then grown for 24 h. The cells were then treated with various concentrations of delphinidin or 0.1% DMSO in DMEM with 1% FBS for 24 h. ARE-luciferase activity was measured with a luciferase activity assay kit (Promega). First, the cells were harvested in reporter lysis buffer. Then, 50 μl of luciferase assay reagent was added to 10 μl of the cell lysate supernatant to catalyze the bioluminescent reaction. The relative luminescence units (RLUs) were quantified using a Sirius luminometer (Berthold Detection System GmbH, Pforzheim, Germany). The readouts were normalized to the protein concentration measured with a BCA protein assay (Pierce Biotech, Rockford, IL, USA). The results are presented as the fold change compared with those for the 0.1% DMSO vehicle control.

Western Blotting

JB6 P+ cells were seeded into 100-mm dishes at a density of 3×10^5 cells/dish and then grown for 24 h. Next, the cells were treated with delphinidin (5, 10, or 20 μM) or 0.1% DMSO in MEM supplemented with 1% FBS for 5 days. The cells were lysed, and the total proteins were extracted with RIPA lysis buffer containing a protease inhibitor cocktail using a sonicator (42). The protein concentrations were measured by the BCA method (Pierce Biotech). Next, 25 μg of protein from each sample was added to the wells of 4 to 15% SDS-PAGE gels (Bio-Rad, Hercules, CA, USA). After electrophoretic separation, the proteins were transferred to a polyvinylidene difluoride (PVDF) membrane (Millipore, Bedford, MA, USA), which was blocked with 5% BSA in TBST to prevent nonspecific binding. Next, the blotting membrane was incubated with different primary antibodies and horseradish peroxidase–conjugated secondary antibodies. Finally, the blot was visualized and photographed with the aid of SuperSignal West Femto–enhanced chemiluminescence substrate (Thermo Fisher Scientific, Waltham, MA, USA) using the Gel Documentation 2000 system (Bio-Rad). The intensities of the signal bands were analyzed with ImageJ software, and the relative protein expression was normalized to that of β-actin. Anti-goat, anti-rabbit, and anti-mouse secondary antibodies were provided by Santa Cruz Biotechnology (Dallas, TX, USA). A primary antibody against β-actin was provided by Santa Cruz Biotechnology, and primary antibodies against Nrf2, NQO1, and HO-1 were obtained from Abcam (Cambridge, MA, USA). Primary antibodies against histone deacetylases (HDACs) (HDAC1, HDAC2, HDAC3, HDAC4, HDAC5, and HDAC7) were supplied by Cell Signaling Technology (Beverly, MA, USA), and primary antibodies against DNA methyltransferases (DNMTs) (DNMT1, DNMT3a, and DNMT3b) were provided by Novus Biologicals (Centennial, CO, USA).

Quantitative Real-Time Polymerase Chain Reaction

JB6 P+ cells were seeded into 100-mm dishes at a density of 3×10^5 cells/dish and then grown for 24 h. Next, the cells were treated with various concentrations of delphinidin (5, 10, or 20 μM) or 0.1% DMSO in MEM with 1% FBS for 5 days. RNA isolation was performed using a GeneJET RNA Purification Kit (Thermo Fisher Scientific). The mRNA expression levels of Nrf2 (*Nfe2l2*) and Nrf2 target genes (*Nqo1*, *Hmox1*, and *Sod-1*) were quantified with an Applied Biosystems 7900HT Fast Real-Time PCR System using the comparative CT (ΔΔCt) method. The relative quantification (RQ) values for the treatment groups were determined compared with the vehicle control (0.1% DMSO) value. The sequences of the forward and reverse primers are as follows: Nrf2: 5′-GGCTCAGCACCTTG TATCTT-3′ and 5′-CACATTGCCATCTCTGGTTTG-3′; NQO1: 5′-GAGAAGAGCCCTGATTGTACTG-3′ and 5′-ACCTCCCATCCTCTCTTCTT-3′; GAPDH: 5′-AACA GCAACTCCCACTCTTC-3′ and 5′-CCTG TTGCTGTAGCCGTATT-3′; HO-1: 5′-CTCC CTGTGTTTCCTTTCTCTC-3′ and 5′-GCTG

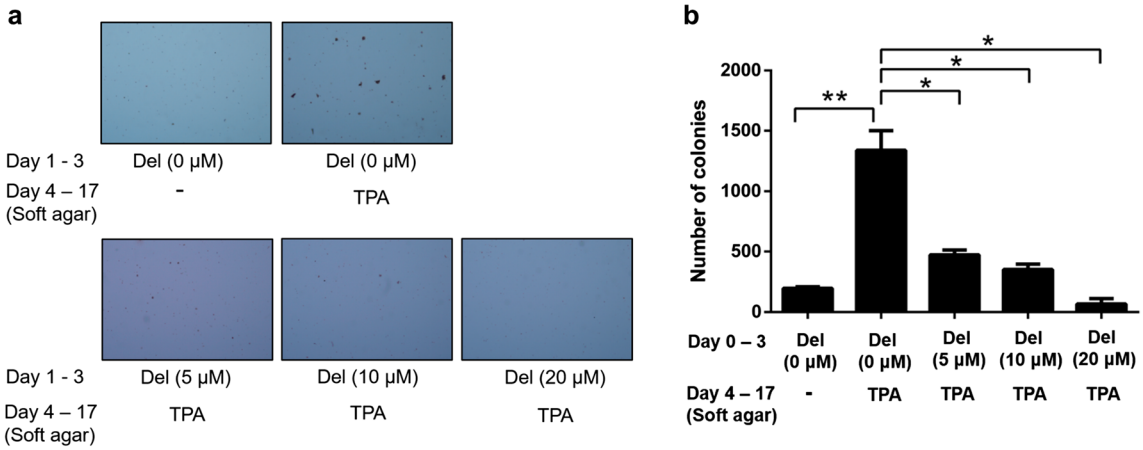

Fig. 2. Inhibitory effects of delphinidin on TPA-induced JB6 P+ cell transformation. JB6 P+ cells (3×10^5/10-cm dish) pretreated with 5, 10, or 20 μM delphinidin for 3 days were transferred to soft agar containing TPA for another 14 days. Then, the colonies showing anchorage-independent growth on soft agar were measured under a microscope and analyzed using ImageJ software. **a** Representative image of transformed JB6 colonies. **b** The statistical data are presented as the mean ± SEM of three replicates from two independent studies. Significant differences were evaluated by Student's *t* test (*$P < 0.05$; **$P < 0.01$)

CTGGTTTCAAAGTTCAG-3′; and SOD1: 5′-GGTT CCACGTCCATCAGTATG-3′ and 5′-GTCT CCAACATGCCTCTCTTC-3′.

Bisulfite Genomic Sequencing

Genomic DNA was extracted from JB6 P+ cells treated with 5, 10, or 20 μM delphinidin or 0.1% DMSO using a GeneJET Genomic DNA Purification Kit (Thermo Fisher Scientific) or a QIAamp DNA Mini Kit (Qiagen, Valencia, CA, USA). A subset of cells was cotreated with 5-aza (250 nM) and TSA (50 nM) as a positive control group; the TSA was only added 20 h before the harvest of cells. The treatment medium was replaced every other day. Next, the isolated DNA was subjected to bisulfite conversion using an EZ DNA Methylation Gold Kit (Zymo Research, Irvine, CA, USA). The methylation level of the 15 CpG sites located between −863 and −1226 nt from the transcription start site in the mouse Nrf2 gene was used as an indicator of Nrf2-ARE pathway activation and cancer development as established in our previous publication (43). The converted DNA fragments were magnified by PCR using Platinum Taq DNA polymerase (Invitrogen). The sequences of the forward and reverse PCR primers are 5′-TTAT AATTTATAGTAATAAAATTAGTTATG-3′ and 5′-CCCATTCAATTACTAATACTCAAACAC-3′. A TOPO TA Cloning Kit (Invitrogen) was used to clone the PCR amplicons into pCR4 TOPO vectors, which were then transformed into One Shot™ TOP10 Chemically Competent *E. coli* (Invitrogen). Finally, 12 colonies from each group were randomly selected and sequenced by GENEWIZ (South Plainfield, NJ, USA).

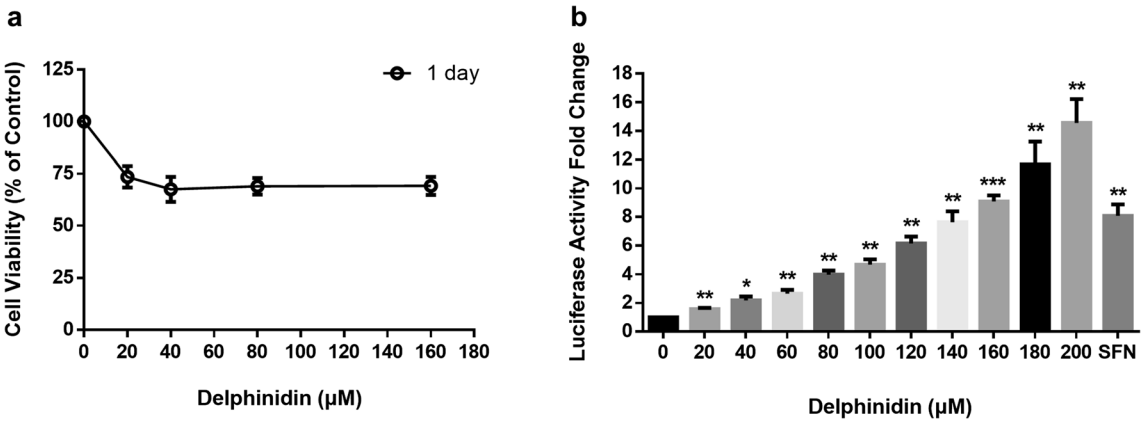

Fig. 3. Effect of delphinidin treatment on cell viability and ARE-luciferase activity in HepG2-C8 cells. **a** The cell viability of HepG2-C8 cells was evaluated after treatment with different concentrations of delphinidin for 1 day. Cell viability was quantified with an MTS assay and is shown as the mean ± SEM. **b** The relative luminescence (in RLU) was normalized to the protein concentrations measured in the BCA protein assay. Sulforaphane (SFN, 5 μM) was used as a positive control. The data are presented as the fold change ± SEM compared with the vehicle control group (0.1% DMSO) value from three independent experiments. *Asterisks* indicate significant differences between the treatment groups and the vehicle control group, as evaluated by Student's *t* test (*$P < 0.05$; **$P < 0.01$; ***$P < 0.001$)

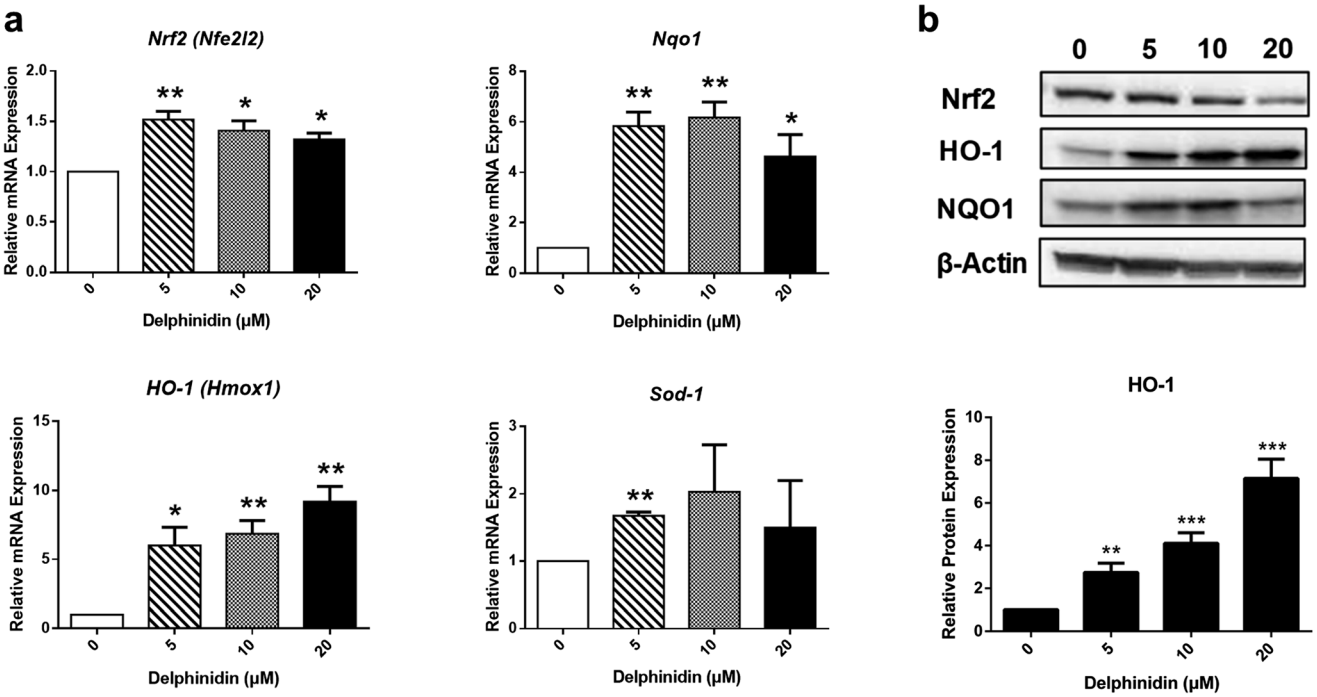

Fig. 4. Effects of delphinidin on the relative endogenous mRNA expression and protein expression of Nrf2 (*NFE2L2*) and Nrf2-targeted ARE genes in JB6 P+ cells. **a** The mRNA expression of Nrf2 (*NFE2L2*), *Nqo1*, *HO-1* (*Hmox1*), and *Sod-1* was measured in JB6 P+ cells following 5-day treatment with different concentrations of delphinidin. The data are presented as the mean ± SEM of three replicates from two independent experiments, and the results for the treatment groups were compared with those of the vehicle control group (0.1% DMSO). **b** The protein expression of Nrf2 (NFE2L2), NQO1, and HO-1 was measured in JB6 P+ cells after 5 days of treatment with various concentrations of delphinidin, and β-actin was used as an internal standard. Densitometric analysis was performed with ImageJ software to quantify the protein expression of at least three independent replicates, which is expressed as the mean ± SEM. The levels in the treatment groups were compared with those in the vehicle control group (0.1% DMSO). Student's *t* test was used to evaluate the significant differences (*$P < 0.05$; **$P < 0.01$; ***$P < 0.001$)

Statistical Analysis

The quantitative results are expressed as the mean ± SEM, and Student's *t* test was applied to evaluate the significance of statistical analysis; * indicates $P < 0.05$, ** indicates $P < 0.01$, *** indicates $P < 0.001$, and **** indicates $P < 0.0001$.

RESULTS

Determination of Delphinidin Concentrations and Duration of Treatments

To determine the optimal concentration and treatment duration, the cytotoxicity of delphinidin was evaluated with an MTS cell proliferation assay. Delphinidin inhibited cell viability in a time- and dose-dependent manner (Fig. 1b). Determination of an ideal treatment duration and concentration involves a trade-off between toxicity and efficacy. The 3-day treatment chosen in this study has been shown to be optimal for observing colony number reductions in cell transformation assays (42,44–52). In addition, a 5-day treatment was chosen for the qPCR studies because this treatment led to more significant differences between the control and treatment groups than 6-h or 3-day treatment (data not shown). A 5-day treatment was used for the western blot studies due to the greater effect observed after 5-day treatment than after 3-day treatment (data not shown). Finally, a 5-day treatment was determined to be optimal for identifying changes in CpG methylation in the Nrf2 promoter in JB6 P+ cells for the bisulfite sequencing study (42,44,45,49). The cell viability after 1- and 3-day delphinidin treatments (< 20 μM) was above 50%, so treatment concentrations of 5, 10, and 20 μM were used in the subsequent mechanistic studies.

Delphinidin Prevents TPA-Mediated JB6 P+ Cell Transformation

The anchorage-independent growth ability of cells in soft agar colony formation assays reflects their neoplastic transformation. TPA, a well-established promoter of skin carcinogenesis both *in vitro* and *in vivo* (53,54), was applied to induce transformation in JB6 P+ cells and was shown to effectively increase colony formation by 7.8-fold compared with the vehicle (Fig. 2). Delphinidin pretreatment significantly attenuated the anchorage-independent growth by 69.4%, 74.4%, and 99.4% in the 5, 10, and 20 μM groups, respectively (Fig. 2). In addition, the number of transformed colonies in the 20 μM group was even less than that in the vehicle control group (Fig. 2). To conclude, the above result indicates that delphinidin can significantly inhibit the TPA-induced anchorage-independent growth of JB6 P+ cells.

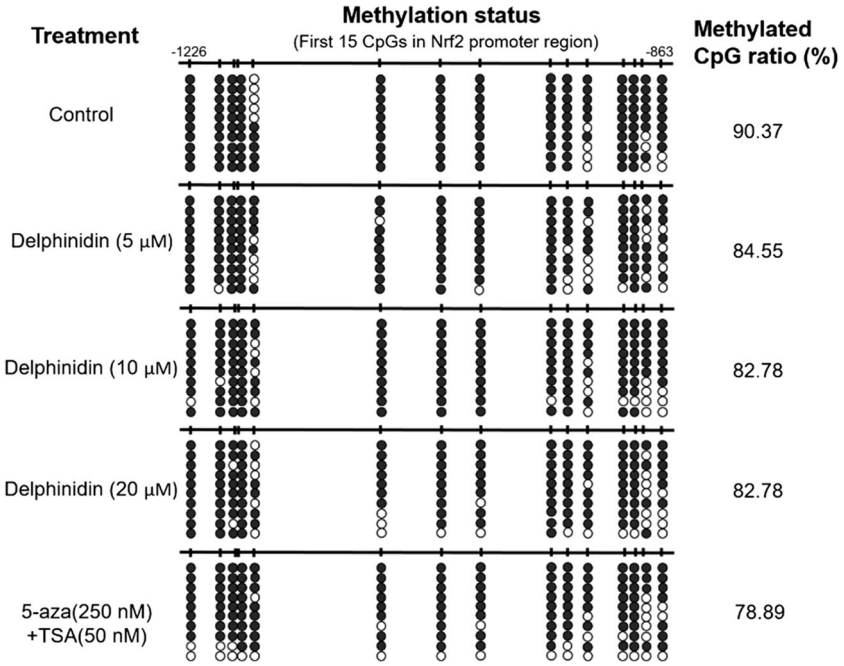

Fig. 5. Effects of delphinidin on the CpG methylation of Nrf2 in JB6 P+ cells. JB6 P+ cells (3×10^5 cells/10-cm dish) were treated with delphinidin for 5 days, and genomic DNA was extracted. Cotreatment with 250 nM 5-azacytidine (5-aza) and 50 nM trichostatin A (TSA) was used as a positive control, but the TSA was only added 20 h before harvesting cells. The DNA methylation profiles of the first 15 CpG sites between nt − 1226 and − 863 in the Nrf2 promoter were determined by bisulfite genomic sequencing, and at least 12 colonies from each group were selected and sequenced using T7 primers. The CpG methylation ratio was evaluated as the percentage of methylated cytosines in the 15 CpG sites for three replicates from two independent experiments and is expressed as the mean ± SEM. The CpG methylation patterns of the sequences of ten colonies randomly chosen from each treatment group are presented. The solid circles indicate the methylated CpG sites, and the open circles represent the unmethylated CpG sites

Delphinidin Enhances ARE-Driven Luciferase Activity

To understand the inhibitory mechanism of delphinidin in cell transformation, HepG2-C8 cells transfected with the pARE-Tl-luciferase reporter construct were used to examine the effect of delphinidin on ARE-driven luciferase activity. Delphinidin increased the normalized RLU in a dose-dependent manner (Fig. 3b). In addition, delphinidin significantly increased ARE-driven luciferase activity compared with the control beginning at 20 μM and exhibited a more potent effect than the positive control, sulforaphane (SFN), at 160 μM (Fig. 3b). The above results suggest that delphinidin may induce the transcription of ARE-dependent genes.

Delphinidin Upregulates the mRNA and Protein Expression of Nrf2 and Its Target Genes

Nrf2 binding to the ARE region can regulate the expression of the carcinogen-detoxifying phase 2 enzymes HO-1 and NQO1 and the reactive oxygen species (ROS) scavenger SOD1 (55). qPCR and western blotting were conducted to understand the activation of the Nrf2-ARE pathway at the mRNA and protein levels in JB6 P+ cells. Five-day delphinidin treatment upregulated the mRNA expression of Nrf2 (*Nfe2l2*) and its target genes (*Hmox1*, *Nqo1*, and *Sod1*) in a dose-dependent manner (Fig. 4a). The protein expression of HO-1 was significantly upregulated by 5-day delphinidin treatment (Fig. 4b), consistent with the mRNA expression results. Taken together, the results suggest that delphinidin can trigger Nrf2-ARE pathways by upregulating antioxidative and carcinogen-detoxifying proteins at the transcriptional and translational levels.

Delphinidin Decreases CpG Methylation in the Nrf2 Promoter Region

To further understand the epigenetic alteration mediated by delphinidin, bisulfite genomic DNA sequencing was performed to evaluate the CpG methylation levels in the Nrf2 promoter region. We previously reported that the 15 CpG sites within − 1226 and − 863 nt of the Nrf2 gene promoter are hypermethylated in prostate TRAMP tumors compared with normal prostate tissues in C57BL/6J mice (43). Moreover, the CpG methylation ratio of the Nrf2 promoter is inversely correlated with the expression of Nrf2 target genes (43). In this study, the vehicle control group had a methylation ratio of 90.37% for the 15 CpG sites in the Nrf2 promoter. Five-day treatment with delphinidin decreased the methylation ratio of these 15 CpG sites to 84.55, 82.78, and 82.78% in the 5 μM, 10 μM, and 20 μM groups, respectively (Fig. 5). The positive control group treated with 5-aza (an inhibitor of DNMTs) and TSA (an inhibitor of HDACs)

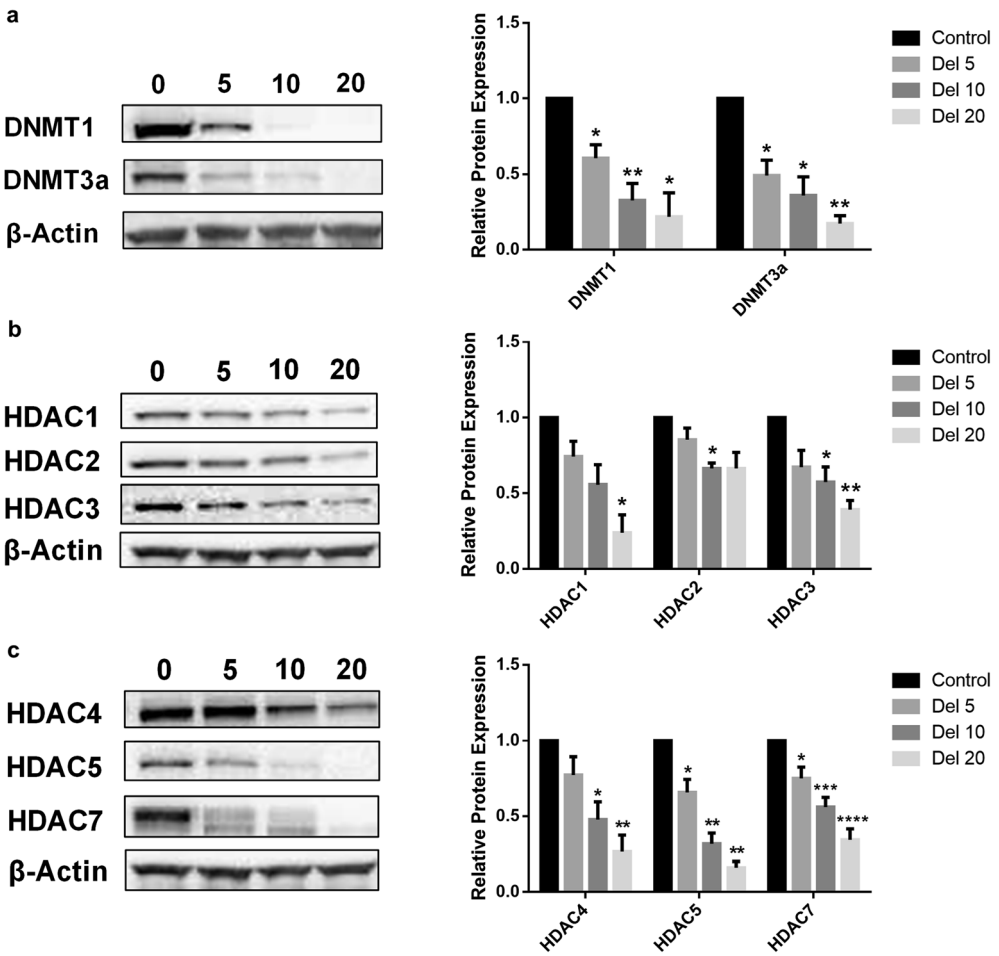

Fig. 6. Effect of delphinidin on the protein expression of **a** DNMTs (DNMT1 and DNMT3a), **b** class I HDACs (HDAC1, HDAC2, and HDAC3) and **c** class II HDACs (HDAC4, HDAC5, and HDAC7) in JB6 P+ cells. Western blotting was conducted following 5-day delphinidin treatment, and β-actin was used as an internal standard. Densitometric analysis was performed with ImageJ software to quantify the protein expression from three independent experiments, which is expressed as the mean ± SEM. Student's *t* test was used to evaluate the significant differences (*$P < 0.05$; **$P < 0.01$; ***$P < 0.001$; ****$P < 0.0001$)

reduced the methylation ratio to 78.89% (Fig. 5), which is consistent with the findings of our previous study (44). In total, the results demonstrate that delphinidin decreases the CpG methylation ratio in the Nrf2 promoter.

Delphinidin Downregulates the Protein Expression of DNMTs and HDACs

The activity of epigenetic modifying enzymes was evaluated to understand the mechanism of DNA demethylation in the Nrf2 promoter. Delphinidin downregulated the protein expression of DNMTs (DNMT1 and DNMT3a) in a dose-dependent manner in JB6 P+ cells (Fig. 6). The decrease in DNMT3b expression caused by delphinidin was not significant (data not shown). The protein expression of HDACs, which have been reported to regulate DNA methylation synergistically with DNMTs (56), was also evaluated in this study. Delphinidin suppressed class I and class II HDACs in a dose-dependent manner after 5 days of treatment. The repression of DNMTs and HDACs was consistent with the decreased CpG methylation in the Nrf2 promoter region, as shown in Fig. 5. These findings suggest that DNMT and HDAC inhibition is a possible molecular mechanism for demethylation of CpG sites in the Nrf2 promoter and reactivation of the Nrf2 pathway.

DISCUSSION AND CONCLUSIONS

The primary prevention of skin cancers involves avoidance of risk factors such as overexposure to UV radiation and chemical pollutants. In situations in which exposure is unavoidable and in individuals with weakened endogenous antioxidative systems due to aging, applying phytochemicals can be a promising strategy for early interference with skin neoplastic development, as these compounds restore homeostasis between the production of ROS and the activity of the antioxidative defense system (57). To understand the effects of phytochemicals and the mechanisms by which they exert their biological activity, systematic study of these compounds at various molecular levels is urgently needed.

In this study, we applied a methodology based mainly on the central dogma of molecular biology. In this methodology, a key cytoprotective pathway involved in cancer development is first selected. Second, an *in vitro* cell transformation model

is designed in which effective carcinogens are applied to initiate cell transformation. Third, the cytoprotective pathway is evaluated with luciferase report assays, qPCR, and western blot analyses to measure gene expression at the transcriptional and translational levels. Finally, epigenetic modifications can be examined by quantifying CpG methylation levels in promoter regions. This methodology can genetically and epigenetically characterize the cancer prevention mechanisms of bioactive compounds to fulfill the need for systematic phytochemical studies.

The ARE is a cis-acting enhancer sequence in the promoter region of various antioxidative genes. Nrf2 can interact with the ARE to activate a variety of antioxidative pathways (58). Nrf2 knockout mice are more susceptible than wild-type mice to chemical carcinogens in various types of cancer models, such as stomach, bladder, and skin cancer models (59). High numbers of skin tumors have been found in Nrf2 knockout mice after exposure to the carcinogens DMBA and TPA (59). Activation of Nrf2 and its target genes, such as *Ho-1* and *Nqo1*, by phytochemicals can block skin cell neoplastic transformation in JB6 P+ cells (39,49). Similarly, in our study, we observed a correlation between inhibition of TPA-mediated anchorage-independent growth and genetic/epigenetic activation of the Nrf2 pathway in JB6 P+ cells. TPA-treated JB6 P+ cells exhibited 7.8-fold greater anchorage-independent growth than vehicle-treated control cells. Pretreatment with delphinidin attenuated the anchorage-independent growth by 69.4%, 74.4%, and 99.4% in the 5 μM, 10 μM, and 20 μM groups, respectively (Fig. 2). The inhibitory mechanism of delphinidin was elucidated by the observed upregulation of ARE-driven luciferase activity, implicating the transcriptional activation of ARE-dependent genes (Fig. 3b). The activation of the Nrf2-ARE pathway was also shown by the increased mRNA and protein expression of the Nrf2 target genes *Ho-1*, *Nqo1*, and *Sod1* (Fig. 4).

We previously reported that hypermethylation in the Nrf2 promoter was associated with prostate cancer progression in 27 clinical prostate cancer samples and in LNCaP cells (60). Moreover, the inhibitory effect of SFN against TPA-induced neoplastic transformation has been found to be regulated by demethylation of the Nrf2 promoter (42). In this study, we examined whether the CpG methylation level in the Nrf2 promoter region was altered by delphinidin to understand the activation of the Nrf2-ARE antioxidative pathway. Five-day delphinidin treatment reduced the methylation levels at the 15 CpG sites between nt − 1226 and − 863 of the Nrf2 gene promoter in a dose-dependent manner in JB6 P+ cells (Fig. 5). Several previous studies have explored how delphinidin regulates histone acetyltransferase (HATs) and HDACs to exert antiinflammatory and apoptosis-inducing effects (61,62). It has been reported that delphinidin can repress inflammatory signaling by specifically inhibiting HATs to downregulate NF-κB acetylation in fibroblast-like synoviocyte MH7A cells (61). In addition, delphinidin could mediate p53-induced apoptosis by specifically inhibiting HDAC3 to activate p53 acetylation in human prostate cancer LNCaP cells (62). In our present study, we found that delphinidin significantly reduced the expression of DNMT1 and DNMT3a as well as class I HDACs (HDAC1, HDAC2, and HDAC3) and class II HDACs (HDAC4, HDAC5, and HDAC7) in JB6 P+ cells (Fig. 6). This result correlates with the observed demethylation of the Nrf2 promoter (Fig. 5). Further studies are needed to understand the overall chemopreventive effects of delphinidin mediated by inhibition of DNMT and HDAC, such as its effects on cell cycle arrest, differentiation, and cell death (63,64).

In conclusion, this study demonstrates that delphinidin, an epigenetic activator of the Nrf2-ARE pathway, inhibits JB6 P+ cell transformation by demethylating 15 CpG sites of the Nrf2 promoter and inhibiting DNMTs and HDACs. The results suggest that delphinidin has the potential to be applied as a skin cancer chemopreventive agent.

ACKNOWLEDGMENTS

This study was supported by R01CA200129 from the National Cancer Institute (NCI). We thank all the members of Dr. Ah-Ng Kong's laboratory for their invaluable discussion and technical support for preparation of this manuscript.

AUTHORSHIP CONTRIBUTIONS

Participated in research design: Hsiao-Chen Dina Kuo and Ah-Ng Kong.

Conducted experiments: Hsiao-Chen Dina Kuo.

Performed data analysis: Hsiao-Chen Dina Kuo, Renyi Wu, Shanyi Li, Anne Yuqing Yang, and Ah-Ng Kong.

Wrote the manuscript: Hsiao-Chen Dina Kuo, Renyi Wu, and Ah-Ng Kong.

COMPLIANCE WITH ETHICAL STANDARDS

Conflict of Interest The authors declare that they have no conflict of interest.

REFERENCES

1. Madan V, Lear JT, Szeimies R-M. Non-melanoma skin cancer. Lancet. 2010;375(9715):673–85.
2. American Cancer Society. Cancer Facts & Figures. Atlanta: American Cancer Society. 2019.
3. Alam M, Ratner D. Cutaneous squamous-cell carcinoma. N Engl J Med. 2001;344(13):975–83.
4. Stewart BW, Kleihues P. editors. World Cancer Report. Lyon: IARC Press. 2003.
5. Slaga TJ, Bracken WM. The effects of antioxidants on skin tumor initiation and aryl hydrocarbon hydroxylase. Cancer Res. 1977;37(6):1631–5.
6. Huang MT, Smart RC, Wong CQ, Conney AH. Inhibitory effect of curcumin, chlorogenic acid, caffeic acid, and ferulic acid on tumor promotion in mouse skin by 12-O-tetradecanoylphorbol-13-acetate. Cancer Res. 1988;48(21):5941–6.
7. Singh RP, Agarwal R. Mechanisms and preclinical efficacy of silibinin in preventing skin cancer. Eur J Cancer. 2005;41(13):1969–79.
8. Huang MT, Ho CT, Wang ZY, Ferraro T, Lou YR, Stauber K, et al. Inhibition of skin tumorigenesis by rosemary and its constituents carnosol and ursolic acid. Cancer Res. 1994;54(3):701–8.
9. Lin BW, Gong CC, Song HF, Cui YY. Effects of anthocyanins on the prevention and treatment of cancer. Br J Pharmacol. 2017;174(11):1226–43.

10. Shih P-H, Yeh C-T, Yen G-C. Anthocyanins induce the activation of phase II enzymes through the antioxidant response element pathway against oxidative stress-induced apoptosis. J Agric Food Chem. 2007;55(23):9427–35.
11. Yi L, Chen C-y, Jin X, Mi M-t, Yu B, Chang H, et al. Structural requirements of anthocyanins in relation to inhibition of endothelial injury induced by oxidized low-density lipoprotein and correlation with radical scavenging activity. FEBS Lett. 2010;584(3):583–90.
12. Esposito D, Chen A, Grace MH, Komarnytsky S, Lila MA. Inhibitory effects of wild blueberry anthocyanins and other flavonoids on biomarkers of acute and chronic inflammation in vitro. J Agric Food Chem. 2014;62(29):7022–8.
13. Peiffer DS, Zimmerman NP, Wang L-S, Ransom B, Carmella SG, Kuo C-T, et al. Chemoprevention of esophageal cancer with black raspberries, their component anthocyanins, and a major anthocyanin metabolite, protocatechuic acid. Cancer Prev Res. 2014;7(6):574.
14. Limtrakul P, Yodkeeree S, Pitchakarn P, Punfa W. Suppression of inflammatory responses by black rice extract in RAW 264.7 macrophage cells via downregulation of NF-kB and AP-1 signaling pathways. Asian Pac J Cancer Prev. 2015;16(10):4277–83.
15. Yoshimoto M, Okuno S, Yoshinaga M, Yamakawa O, Yamaguchi M, Yamada J. Antimutagenicity of sweetpotato (Ipomoea batatas) roots. Biosci Biotechnol Biochem. 1999;63(3):537–41.
16. Shi MZ, Xie DY. Biosynthesis and metabolic engineering of anthocyanins in Arabidopsis thaliana. Recent Pat Biotechnol. 2014;8(1):47–60.
17. Hou D-X, Fujii M, Terahara N, Yoshimoto M. Molecular mechanisms behind the chemopreventive effects of anthocyanidins. Biomed Res Int. 2004;2004(5):321–5.
18. Veberic R, Slatnar A, Bizjak J, Stampar F, Mikulic-Petkovsek M. Anthocyanin composition of different wild and cultivated berry species. LWT-Food Sci Technol. 2015;60(1):509–17.
19. Simon JE, Morales MR, Phippen WB, Vieira RF, Hao Z. Basil: a source of aroma compounds and a popular culinary and ornamental herb. In: Janick J, editors. Fourth National Symposium New Crops and New Uses: Biodiversity and Agricultural Sustainability; Perspectives on New Crops and New Uses; 1998; Phoenix, AZ. Alexandria: ASHS Press; 1999. p. 499–505.
20. Awika JM, Rooney LW, Waniska RD. Anthocyanins from black sorghum and their antioxidant properties. Food Chem. 2005;90(1):293–301.
21. Li C-Y, Kim H-W, Won SR, Min H-K, Park K-J, Park J-Y, et al. Corn husk as a potential source of anthocyanins. J Agric Food Chem. 2008;56(23):11413–6.
22. Srivastava J, Vankar PS. Canna indica flower: new source of anthocyanins. Plant Physiol Biochem. 2010;48(12):1015–9.
23. Ichikawa H, Ichiyanagi T, Xu B, Yoshii Y, Nakajima M, Konishi T. Antioxidant activity of anthocyanin extract from purple black rice. J Med Food. 2001;4(4):211–8.
24. Aguilera Y, Mojica L, Rebollo-Hernanz M, Berhow M, de Mejía EG, Martín-Cabrejas MA. Black bean coats: new source of anthocyanins stabilized by β-cyclodextrin copigmentation in a sport beverage. Food Chem. 2016;212:561–70.
25. Pazmiño-Durán EA, Giusti MM, Wrolstad RE, Glória MBA. Anthocyanins from banana bracts (Musa X paradisiaca) as potential food colorants. Food Chem. 2001;73(3):327–32.
26. Hou D-X, Kai K, Li J-J, Lin S, Terahara N, Wakamatsu M, et al. Anthocyanidins inhibit activator protein 1 activity and cell transformation: structure–activity relationship and molecular mechanisms. Carcinogenesis. 2004;25(1):29–36.
27. Zhao Y, Xue Y, Oberley TD, Kiningham KK, Lin S-M, Yen H-C, et al. Overexpression of manganese superoxide dismutase suppresses tumor formation by modulation of activator protein-1 signaling in a multistage skin carcinogenesis model. Cancer Res. 2001;61(16):6082–8.
28. Afaq F, Syed DN, Malik A, Hadi N, Sarfaraz S, Kweon M-H, et al. Delphinidin, an anthocyanidin in pigmented fruits and vegetables, protects human HaCaT keratinocytes and mouse skin against UVB-mediated oxidative stress and apoptosis. J Investig Dermatol. 2007;127(1):222–32.
29. Ma Q. Role of Nrf2 in oxidative stress and toxicity. Annu Rev Pharmacol Toxicol. 2013;53(1):401–26.
30. Chan JY, Cheung MC, Moi P, Chan K, Kan YW. Chromosomal localization of the human NF-E2 family of bZIP transcription factors by fluorescence in situ hybridization. Hum Genet. 1995;95(3):265–9.
31. Jaramillo MC, Zhang DD. The emerging role of the Nrf2-Keap1 signaling pathway in cancer. Genes Dev. 2013;27(20):2179–91.
32. Deshmukh P, Unni S, Krishnappa G, Padmanabhan B. The Keap1-Nrf2 pathway: promising therapeutic target to counteract ROS-mediated damage in cancers and neurodegenerative diseases. Biophys Rev. 2017;9(1):41–56.
33. Furukawa M, Xiong Y. BTB protein Keap1 targets antioxidant transcription factor Nrf2 for ubiquitination by the Cullin 3-Roc1 ligase. Mol Cell Biol. 2005;25(1):162–71.
34. Taguchi K, Motohashi H, Yamamoto M. Molecular mechanisms of the Keap1-Nrf2 pathway in stress response and cancer evolution. Genes Cells. 2011;16(2):123–40.
35. Singh S, Vrishni S, Singh BK, Rahman I, Kakkar P. Nrf2-ARE stress response mechanism: a control point in oxidative stress-mediated dysfunctions and chronic inflammatory diseases. Free Radic Res. 2010;44(11):1267–88.
36. Hu R, Saw CL, Yu R, Kong AN. Regulation of NF-E2-related factor 2 signaling for cancer chemoprevention: antioxidant coupled with antiinflammatory. Antioxid Redox Signal. 2010;13(11):1679–98.
37. Kansanen E, Kuosmanen SM, Leinonen H, Levonen AL. The Keap1-Nrf2 pathway: mechanisms of activation and dysregulation in cancer. Redox Biol. 2013;1:45–9.
38. Roslin JT, Deepak B, Kendra FB, Erzsebet H-R, Judit H, Altaf SD, et al. Black currant anthocyanins abrogate oxidative stress through Nrf2-mediated antioxidant mechanisms in a rat model of hepatocellular carcinoma. Curr Cancer Drug Targets. 2012;12(9):1244–57.
39. Yang Y, Yang I, Cao M, Su ZY, Wu R, Guo Y, et al. Fucoxanthin elicits epigenetic modifications, Nrf2 activation and blocking transformation in mouse skin JB6 P+ cells. AAPS J. 2018;20(2):32.
40. Yu R, Lei W, Mandlekar S, Weber MJ, Der CJ, Wu J, et al. Role of a mitogen-activated protein kinase pathway in the induction of phase II detoxifying enzymes by chemicals. J Biol Chem. 1999;274(39):27545–52.
41. Kim H, Ramirez CN, Su ZY, Kong AN. Epigenetic modifications of triterpenoid ursolic acid in activating Nrf2 and blocking cellular transformation of mouse epidermal cells. J Nutr Biochem. 2016;33:54–62.
42. Su ZY, Zhang C, Lee JH, Shu L, Wu TY, Khor TO, et al. Requirement and epigenetics reprogramming of Nrf2 in suppression of tumor promoter TPA-induced mouse skin cell transformation by sulforaphane. Cancer Prev Res (Phila). 2014;7(3):319–29.
43. Yu S, Khor TO, Cheung KL, Li W, Wu TY, Huang Y, et al. Nrf2 expression is regulated by epigenetic mechanisms in prostate cancer of TRAMP mice. PLoS One. 2010;5(1):e8579.
44. Paredes-Gonzalez X, Fuentes F, Su Z-Y, Kong A-NT. Apigenin reactivates Nrf2 anti-oxidative stress signaling in mouse skin epidermal JB6 P + cells through epigenetics modifications. AAPS J. 2014;16(4):727–35.
45. Khor TO, Huang Y, Wu T-Y, Shu L, Lee J, Kong A-NT. Pharmacodynamics of curcumin as DNA hypomethylation agent in restoring the expression of Nrf2 via promoter CpGs demethylation. Biochem Pharmacol. 2011;82(9):1073–8.
46. Wu T-Y, Khor TO, Su Z-Y, Saw CL-L, Shu L, Cheung K-L, et al. Epigenetic modifications of Nrf2 by 3,3′-diindolylmethane in vitro in TRAMP C1 cell line and in vivo TRAMP prostate tumors. AAPS J. 2013;15(3):864–74.
47. Huang Y, Khor TO, Shu L, Saw CL-L, Wu T-Y, Suh N, et al. A γ-tocopherol-rich mixture of tocopherols maintains Nrf2 expression in prostate tumors of TRAMP mice via epigenetic inhibition of CpG methylation. J Nutr. 2012;142(5):818–23.
48. Zhang C, Su Z-Y, Khor TO, Shu L, Kong A-NT. Sulforaphane enhances Nrf2 expression in prostate cancer TRAMP C1 cells through epigenetic regulation. Biochem Pharmacol. 2013;85(9):1398–404.
49. Wang L, Zhang C, Guo Y, Su Z-Y, Yang Y, Shu L, et al. Blocking of JB6 cell transformation by Tanshinone IIA:

epigenetic reactivation of Nrf2 antioxidative stress pathway. AAPS J. 2014;16(6):1214–25.
50. Su Z-Y, Khor TO, Shu L, Lee JH, Saw CL-L, Wu T-Y, et al. Epigenetic reactivation of Nrf2 in murine prostate cancer TRAMP C1 cells by natural phytochemicals Z-Ligustilide and Radix Angelica Sinensis via promoter CpG demethylation. Chem Res Toxicol. 2013;26(3):477–85.
51. Vaid M, Prasad R, Singh T, Jones V, Katiyar SK. Grape seed proanthocyanidins reactivate silenced tumor suppressor genes in human skin cancer cells by targeting epigenetic regulators. Toxicol Appl Pharmacol. 2012;263(1):122–30.
52. Wang L-S, Kuo C-T, Cho S-J, Seguin C, Siddiqui J, Stoner K, et al. Black raspberry-derived anthocyanins demethylate tumor suppressor genes through the inhibition of DNMT1 and DNMT3B in colon cancer cells. Nutr Cancer. 2013;65(1):118–25.
53. Wei S-J, Trempus CS, Ali RC, Hansen LA, Tennant RW. 12-O-tetradecanoylphorbol-13-acetate and UV radiation-induced nucleoside diphosphate protein kinase B mediates neoplastic transformation of epidermal cells. J Biol Chem. 2004;279(7):5993–6004.
54. Abel EL, Angel JM, Kiguchi K, DiGiovanni J. Multi-stage chemical carcinogenesis in mouse skin: fundamentals and applications. Nat Protoc. 2009;4(9):1350–62.
55. Zhang Y, Gordon GB. A strategy for cancer prevention: stimulation of the Nrf2-ARE signaling pathway. Mol Cancer Ther. 2004;3(7):885–93.
56. Arzenani MK, Zade AE, Ming Y, Vijverberg SJ, Zhang Z, Khan Z, et al. Genomic DNA hypomethylation by histone deacetylase inhibition implicates DNMT1 nuclear dynamics. Mol Cell Biol. 2011;31(19):4119.
57. Godic A, Poljšak B, Adamic M, Dahmane R. The role of antioxidants in skin cancer prevention and treatment. Oxid Med Cell Longev. 2014;2014(5):860479
58. Raghunath A, Sundarraj K, Nagarajan R, Arfuso F, Jinsong B, Kumar AP, et al. Antioxidant response elements: discovery, classes, regulation and potential applications. Redox Biol. 2018;17:297–314.
59. Xu C, Huang M-T, Shen G, Yuan X, Lin W, Khor TO, et al. Inhibition of 7, 12-dimethylbenz (a) anthracene-induced skin tumorigenesis in C57BL/6 mice by sulforaphane is mediated by nuclear factor E2–related factor 2. Cancer Res. 2006;66(16):8293–6.
60. Khor TO, Fuentes F, Shu L, Paredes-Gonzalez X, Yang AY, Liu Y, et al. Epigenetic DNA methylation of antioxidative stress regulator NRF2 in human prostate cancer. Cancer Prev Res (Phila). 2014;7(12):1186–97.
61. Seong AR, Yoo JY, Choi K, Lee MH, Lee YH, Lee J, et al. Delphinidin, a specific inhibitor of histone acetyltransferase, suppresses inflammatory signaling via prevention of NF-kappaB acetylation in fibroblast-like synoviocyte MH7A cells. Biochem Biophys Res Commun. 2011;410(3):581–6.
62. Jeong M-H, Ko H, Jeon H, Sung G-J, Park S-Y, Jun WJ, et al. Delphinidin induces apoptosis via cleaved HDAC3-mediated p53 acetylation and oligomerization in prostate cancer cells. 2016;7(35):56767.
63. Eckschlager T, Plch J, Stiborova M, Hrabeta J. Histone deacetylase inhibitors as anticancer drugs. Int J Mol Sci. 2017;18(7):1414.
64. Medina-Franco JL, Yoo J, Dueñas-González A. Chapter 13—DNA methyltransferase inhibitors for cancer therapy. In: Zheng YG, editor. Epigenetic Technological Applications. Boston: Academic Press; 2015. p. 265–90.